Fractured Basement Reservoir Characterization for Fracture Distribution, Porosity and Permeability Prediction*

Marie Lefranc[1], Sherif Farag[1], Laurent Souche[1], and Agnes Dubois[1]

Search and Discovery Article #41106 (2012)
Posted December 31, 2012

*Adapted from extended abstract prepared in conjunction with oral presentation at AAPG International Conference and Exhibition, Singapore, September 16-19, 2012,

[1]Schlumberger, Ho Chi Minh City, Vietnam (mailto:mlefranc@slb.com)

Abstract

Fractured basement reservoirs are challenging to model due to the complexity of processes involved in the generation and preservation of the fracture network as well as the heterogeneity of the host rock. This study demonstrates an integrated approach to model these unconventional reservoirs through the application of continuous fracture modeling (CFM) and discrete fracture network modeling (DFN). The main objectives of this workflow are to identify the potential flow contributing fractures and to reduce economic risks by optimizing the identification of new well targets.

The first step in this workflow is to minimize the uncertainty in the identification of flow contributing fracture sets, which are estimated from: (1) the analyses of borehole images, sonic measurements, conventional log data, production and mud log data, (2) the laterolog resistivity, and (3) the semi-automated fracture trace extraction analysis generating P33 log (volume of fractures per volume of rock). Once the correlation between these three fracture indicators has been validated, the fracture intensity can be populated in the inter-well space.

The next step is the selection of 3D properties that can be used to propagate the fracture flow indicator away from the wells. Fracture „drivers" used here are optimized post-stack seismic attributes (including Ant-Tracking), seismic inversion data and optimized 3D forward geomechanical properties. Then, 3D fracture intensity models (CFM) are constructed using a method based on artificial neural network methods (ANN).

Finally, fracture properties are computed through DFN modeling. An advanced workflow was created to accurately estimate: fracture distribution, geometry and orientation with well data calibration. The DFN scale-up is then performed through a novel combination of Oda and flow-based methods that allow obtaining 3D porosity and permeability distribution. It is ensured that the scaled-up DFN model can

reproduce dynamic reservoir history such as that from well tests and production logs. The final calibrated model can be used to predict the flow rates and recovery of prospective wells.

Introduction

Naturally fractured reservoirs have been classified according to the relative contribution of the matrix and fractures to the total fluid production (Nelson, 2001). The different types of fractured reservoirs are: (1) Type 1 - Fractures provide essential porosity and permeability, (2) Type 2 - Fractures provide essential permeability, and (3) Type 3 - Fractures provide permeability assistance. Fractured basement reservoirs differ from other types of naturally fractured reservoirs in that they are generally considered to have no primary porosity (Le Van Hung et al., 2009) and are considered to be type 1 reservoirs. The most difficult problem after finding basement rock reservoirs is to evaluate them, particularly their production capacity and their reserves (Luthi, 2005). Often, in this environment, the majority of the wells drilled are highly deviated or horizontal, and drilled to intersect sub-vertical fault zones. To be productive, a well in this environment should encounter enough larger, permeable fractures which are sufficiently connected to the storage capacity of the reservoir (Le Van Hung et al., 2009).

Our approach to continuous fracture modeling (CFM) is a method of 3D fracture modeling that maximizes the geosciences controls on predicting fracture intensity in the interwell space. The objective of the method is to identify the large permeable fractures which are necessary for a well to be productive and to model the fracture density in 3D using optimized fracture set(s) and optimized 3D parameters.

In this article we describe the methods for detailed and robust analysis of borehole images. We also present a quantitative approach to select the fracture drivers from seismic and explain the method used to extend this information to the whole volume. The fracture model presented also uses geomechanical methods to predict the secondary deformation characteristics such as density and orientation of faults and joints. These outputs are combined with the fracture drivers from the seismic to build the fracture density model. Finally we discuss the discrete fracture network (DFN) modeling and the DFN and IFM upscaling which are the key steps in generating the properties describing fracture permeability and porosity.

Fracture Classification and Interpretation

Literature review reveals many examples of fracture classification in basement reservoirs. Each author advocates a different approach based on either descriptive morphologic criteria, such as continuous, discontinuous, solution enhanced fractures (vuggy), brecciated, etc. (Li et al., 2004), or subjective aperture criteria, such as mega, major and minor and fracture density distribution function analysis (Tamagawa and Tezuka, 2004), or even both morphologic and aperture criteria combined (Tandom et al., 1999). Even if the fracture classifications are similar and tend to achieve the same objective, the definitions vary from one author to the next. Moreover, the assignment of morphologic criteria to a fracture is sometimes ambiguous on the image log. The reliability and consistency of fracture classification and interpretation will have significant impact on the fracture density curves used as basis for further analysis with other geological, geomechanical, and geophysical data. Since the fracture density data form the foundation of the characterization and modeling input, it is imperative to rely on good fracture density data and ensure that a reliable correlation with production indicators or flow zones is established before carrying it further into the modeling domain. The main issue with borehole image interpretation in the basement is: how can a „standard" and consistent fracture classification and interpretation be achieved?

Among the possible solutions, we retained all the electrically conductive fractures (without differentiation between continuous, discontinuous and solution enhanced) and the results from another method based on recent research efforts and software development - the semi-automated fracture trace extraction method. This solution is based on image analysis principles applied to borehole images logs. The advantages of this method are the tremendous time savings and improved accuracy of fracture detection, which makes the interpretation results more objective and consistent along the borehole and fully repeatable. Segments extracted automatically from the image logs are synchronized with a stereonet, which enables working with and analyzing data by fracture sets. Upfront definition of classes of open fractures is not necessary. Based on our observation in the basement, the only and single necessary classification applied is the identification of drilling-induced fractures and differentiating them from natural fractures.
This new approach discussed above has been tested on and evaluated with data from several wells from Vietnam and has been carried through a full analysis against indicators of flow or productive zones in the basement.

Fracture Data Analysis

Fracture data analysis is the second step in the reservoir characterization and modeling workflow. It consists of the determination of the types of fractures or fracture parameters that control the distribution and quality of flow zones. In our studies, we took three quantitative approaches which are described below:

Method 1: Determination of the Fracture Indicator from Borehole Images, Sonic and Production Data

After an objective and consistent interpretation of borehole images data is achieved, a detailed analysis of the fracture parameters versus production data (e.g. PLT) is required to identify a variable or a set of variables such as dip, azimuth, aperture, or density, controlling hydrocarbon flow. Fracture indicators such as production rates, index, production logging data, and Stoneley waveform analysis from sonic measurements, are combined with borehole images to flag the flow-contributing fracture zones. These measurements are defined as fracture indicators. This first technique has been used successfully in the past in the fractured basement from Vietnam (Tandom et al., 1999; Li et al., 2004; Luthi, 2005).

The first criterion to identify fracture sets is based on the fractures dip and azimuth. Several conventional diagrams are useful for defining the orientation distribution of fracture populations.

The second criterion is based on fractures aperture. For example, for a specific case study from Vietnam, we took a quantitative approach in which resistivity-derived fracture aperture is used as an objective criterion to distinguish fractures. The combination with the aperture criteria offers quantitative parameterization to identify and select flow-contributing fractures for definition of reservoir intervals.

The third criterion includes: (1) the caliper, which shows a slight enlargement in front of a fracture, (2) the deep and shallow resistivity logs that might show a separation larger than usual, (3) the barium in the drilling mud, which might invade a fracture and result in a higher photoelectric absorption or density reading (Narr et al., 2006), (4) the dipmeter tool rotation which can slow down, and (5) the sonic velocities (Donald and Bratton, 2006; Endo et al., 1998). The set of fractures interpreted from log images is then compared qualitatively to the sonic measurements (Stoneley parameters) which provide a technique for evaluating the morphology and the permeability of fractures and compared with production data to identify and separate the fracture data into sets.

Once the set of flow-contributing fractures has been identified, it is used in the form of a fracture intensity curve (Figure 1). Generation of intensity logs from fracture data is essential in the data analysis because the intensity curve describes the density of fractures per unit length and provides an input fracture distribution for the CFM. The intensity log is a virtual log connected to the interpreted fractures so that the data used in creating the log can be filtered during data analysis.

Method 2: Determination of the Fracture Indicator from the Segment Extracted from the Semi-automatic Fracture Trace Extraction

The workflow and benefits of fracture segment extraction are different from traditional fracture picking with sinusoids. Sinusoid fracture picking focuses on planar fractures. Fracture orientation analysis is properly addressed but fracture densities are highly dependent on the picking practice of the user. Fracture segment extraction detects all features regardless of their planarity. Fracture segment extraction is automated so long and short fractures are fully depicted.

Consequently, fracture densities are more thoroughly computed even for non-planar features. As in the sinusoid-based method, fracture orientations are also computed. The extraction of segment in the image is based on morphology operations. Mathematical morphology is a non-linear theory that provides a tool for investigating geometric structure in images. Its objective is to analyze objects in the image according to their shape, their size, their neighborhood relationship, and their gray scale values. This approach is extremely efficient to solve problems that require shape analysis with speed constraints. Applying morphology operations, followed by a curve-fitting algorithm, a set of curves (polygonal lines) is extracted from the input image.

In the case of drilling-induced fractures, the manual classification can be unreservedly used in the stereonet plot; this method provides a quick way to identify isolated clusters and quickly classify the concerning numerous segments in the segment set corresponding to drilling-induced fractures.

From the semi-automatic fracture trace extraction, different fracture densities can be extracted including:

1) P10 is the number of fractures (defined as segment groups) by unit length of borehole (inverse length unit),

2) P10C is the number of fractures (defined as segment groups) by unit length of borehole corrected for the orientation bias (i.e. angle between each planar fracture and the borehole axis) (inverse length unit),

3) P21is the fracture (defined as segment group) length per unit area of borehole surface (inverse length unit),

4) P30 is the number of fractures (defined as segment groups) per unit volume of borehole rock volume (inverse volume unit),

5) P32 is the fracture (defined as segment group) area per unit volume of borehole rock volume (inverse length unit),

6) P33 is the fracture (defined as segment group) volume per unit volume of borehole rock volume (porosity unit).

From the different case studies performed in fractured basement reservoirs, it appears that the aperture is an important criterion to identify the flow-contributing fractures. The computation of the P32 log does not consider the aperture, whereas aperture is used to compute the P33 log. This P33 density is the second fracture indicator used in our workflow. This new method has been tested in Vietnam and also in Yemen. Field data from basement reservoirs in Yemen show good correlations between the P33 density (fracture porosity) and the productive zones.

Method 3: Determination of the Fracture Indicator from Laterolog Resistivity

One of the limitations of image logs is that they can be sensitive to bad hole conditions. Unfortunately, large fracture zones tend to be associated with borehole damage. To assist with the image interpretation, fracture aperture is also estimated from laterolog resistivity (Faivre, 1993; Sibbit, 1995; Wang et al., 1998). The cumulative fracture aperture over the measurement resolution of the tool is calibrated to match the image-based fracture aperture where the image data is reliable. The laterolog has good tolerance to bad hole conditions in a low-porosity-matrix environment, so it complements image-based fracture aperture where the borehole is poor. It also provides a continuous fracture aperture estimate which includes all the electrically conductive fractures, including those which are too small, or too numerous to be accurately picked on the image logs.

In this method (Hung et al., 2009), sonic logs are used to help in differentiating between permeable and clay-filled fractures. The Stoneley and dipole attenuation measurements are combined with the fracture aperture computed from resistivity (Figure 2). The fracture indicators from Stoneley measurements are affected by bad borehole, so it can be difficult to differentiate between a highly fractured zone from a bad hole. The dipole attenuation is much less affected by bad hole conditions, but is affected by dykes and lithology boundaries.

All the fracture indicators discussed in this third method tend to be overly optimistic (prone to false positive fracture indication), but have different sensitivities to the borehole and lithology variation. On the other hand, none of these indicators are prone to false negative fracture indication. If any of the measurements indicates that there are no large aperture fractures, then it is very likely to be true. The petrophysical interpretation starts with either the resistivity, or image-derived apertures and eliminates all fractures not detected by both the Stoneley and dipole attenuation. This simple technique has proven to be very effective in isolating the large aperture, fluid-filled, fractures (Figure 3).

Combination of Results from the Three Different Approaches

The final step of the data analysis part of the workflow is a qualitative check and development of a quantitative correlation between the different indicators of flow-contributing fractures (Figure 4). The analysis of the fracture intensity (Method 1), P33 (Method 2), and flow indicator from laterolog resistivity (Method 3) shows in our example that these three fracture indicators are correlated both qualitatively and quantitatively. Once the correlation between the fracture indicators has been checked and validated, the fracture intensity can be used for modeling in the interwell space.

Prediction of the Fracture Intensity in the Interwell Space

The next step of the fracture data analysis consists of using the identified fracture set in the form of fracture intensity curve as a fracture flow indicator and finding a possible set of 3D properties that can be used to propagate the fracture flow indicator away from the wells. In this workflow, we evaluate all possible fracture drivers, defined as any 3D property that can be sensitive to or directly or indirectly captures fracture intensity information in the interwell space. Fracture drivers used in our workflow are post-stack seismic attributes, prestack seismic attributes, seismic inversion data and 3D forward geomechanical properties.

Identification of the Best Fracture Drivers

Post-stack Seismic Attributes

The most frequently used fracture drivers in the case studies performed in Vietnam are post-stack seismic attributes. These include:

- Attributes derived from edge detection and direct fault/fracture detection of seismic discontinuity analysis and image processing techniques, which attributes include: variance, chaos, dip deviation, and ant tracking.

- Structural seismic attributes: flatness and curvature.

- Spectral attributes: seismic attributes that capture the frequency content of the seismic data. It is well known that distribution of fractures impact the frequency content of the seismic data by differential attenuation compared to intervals with no or fewer fractures. These attributes include: iso frequency attributes and T*attenuation attributes.

- Post-stack inversion attributes such as acoustic impedance and relative acoustic impedance.

Ant tracking is a patent-protected technology (Figure 5) from Schlumberger that performs edge enhancement for the identification of faults, fractures and other linear anomalies within the seismic data volume. Swarm intelligence concepts are used for introducing a high number of agents (ants) into the data volume and evaluating the collective behavior of the swarm (Randen et al., 2001; Pedersen et al., 2002). Most of the time, this approach gives successful results in naturally fractured reservoirs for populating the fracture intensity in the inter-well space.

This workflow enables us to consider and weigh all possible fracture drivers that are extracted along the existing borehole in the form of a pseudo-log. These pseudo-logs of seismic attributes are then used as input to a multi-scale statistical correlation analysis in which fracture flow indicators/intensity curves are compared to seismic attributes (Figure 6). Because the seismic domain comes with inherent resolution limitations compared to borehole data, a multi-scale analysis is required. The fracture flow indicator in the form of fracture intensity curves is generated with different window filter sizes to evaluate the best scaling factor for optimizing the correlation with the seismic domain.

Geomechanical Attributes

The 3D seismic data in fractured basement reservoirs can sometimes be challenging to interpret and allow identifying only the main faults affecting the naturally fractured reservoirs. Moreover, natural fractures such as small-scale faults and joints are known to be capable of significantly altering the flow of hydrocarbons and are below the resolution of the seismic data in this type of environment. Maerten, 2000, and Maerten et al., 1999 and 2006 demonstrate how geomechanical models based on elastic dislocation can be applied to improve the interpretation understanding and obtain more realistic reservoir models.

Fractures form because rock cannot sustain the in-situ stress and are oriented according to the direction of principal stress. Tensile fractures propagate in a surface normal to the local direction of maximum tensile stress, and shear fractures propagate in one of the two surfaces parallel to the local direction of the intermediate principal stress and at a fixed angle to the local direction of most compressive stress (Bourne and Willemse, 2001). Once open, tensile fractures open in the direction of the least compressive stress and propagate perpendicular to this direction. Therefore, knowledge of the distribution of stress magnitude and direction throughout a rock body can be used to predict the distribution and orientation of fractures.

The stress field responsible for reservoir fracturing can be calculated using geomechanics. Brittle fractures form where this stress field exceeds the local material strength as characterized by the brittle failure envelope for both tensile and shear fractures (Bourne et al., 2000). Poly3D is a 3D boundary element program and its graphic user interface written to calculate the displacements, strains and stresses in an elastic whole- or half-space using planar, polygonal-shaped elements of displacement discontinuity (Figure 7). Poly3D solves the equations of linear elasticity by representing fault surfaces with a series of triangle elements, each of constant slip. Geologically, a polygonal element may represent some portion, or all, of a fracture or fault surface. Because the displacement discontinuity (joint aperture or fault slip) is constant on each element, one can use more than one element to model a fracture or fault with a non-uniform opening and/or slip distribution. Elements also may be joined together to form a closed surface. The discretization of a three-dimensional fault surface into polygonal boundary elements allows the construction of a surface with any desired tipline shape. Boundary conditions, i.e. displacement discontinuities or tractions, can be prescribed locally at the center of each element according to the local coordinate system attached to the element. Additionally, remote stresses and/or strains can be prescribed. Outputs at observation points can be displacements, stain, stress, principal strain and/or principal stresses (Maerten, 2010).

The methodology to model subsurface small-scale fractures consists of calculating the stress distribution at the time of the fracturing using the available reservoir data such as faults, fractures and fold, rock properties and tectonic settings that can be characterized by stress or strain magnitude and orientation. Geomechanical models are created to calibrate the 3D structural model, the applied tectonic loads, and the boundary conditions. Based on the first results, a second set of models are created to predict the secondary deformation characteristics (i.e. density and orientation of fractures). The results are then compared with the fracture data available along the wells.

Remark

The two main factors that allow quantitative modeling of fracture reactivation are the geometry of pre-existing natural fractures and the present day perturbed stress (Maerten, 2010). As it was shown by Tamagawa and Pollard (2008) in fractured basement reservoir from Yufutsu Field, Japan, non-productive wells were drilled in the area where the regional stress prevails, and the most productive well penetrated the area near the tips of active faults, where the stress concentration leads to enhancements in fracture permeability by opening and shearing. The prediction of fracture reactivation under the present day stress field is part of the workflow presented here.

Fracture Intensity Prediction

In the end, all possible fracture drivers - seismic attributes and geomechanical properties - are compared simultaneously and quantitatively with fractures flow indicators, along the wells, having different filtering scale parameters. From that analysis, the best possible fracture drivers are selected.

Neural networks are then used to define the relationships between the ensemble of high-ranked drivers, here ant tracking and flatness (Figure 8), considered in the previous example as best fracture drivers, by finding the underlying complex relationships that exist between the fracture indicator and fracture drivers at the wells. The output of the artificial neural network is an estimated fracture intensity property in 3D space. The final modeling step consists of using the estimated fracture intensity 3D property as an input to collocated co-kriging and sequential gaussian simulation to generate a three-dimensional fracture intensity model that fully honors well data (Figure 8). By combining multiple realizations, probability or confidence maps are constructed to predict those parts of the reservoir that are most intensely fractured. Based on this result, new well targets and optimized well paths can be defined.

Permeability and Porosity Modeling

DFN Modeling

The second step of the fracture modeling process is the fracture network modeling. In our workflow, the description of fractured basement reservoir relies on DFN and IFM (implicit fracture modeling) modeling as shown in Figure 9 (Souche et al., 2009). The DFN model represents fractures, joints and faults as planar surfaces in three dimensions. The DFN (large reservoir-scale fractures) representation has the following advantages: (1) it provides a geologically sound representation based on physically measurable parameters (fracture orientation, length, aperture) and the means for upscaling is to a dual medium model that can be simulated using traditional finite difference simulators, (2) it allows representing large elements such as faults or fracture corridors that span through several simulation grid blocks and therefore to assess the large scale connectivity of the reservoir, (3) it is a stochastic representation that can be used to estimate the uncertainty and the heterogeneity of the output variables (fracture porosity, permeability, etc.). Since the input parameters (fracture density, orientation) are 3D properties, it also captures the variability of these variables at the reservoir scale.

The implicit fracture model (small-scale) is a model of a fracture network in which each of the parameters necessary to describe the geometry and the properties of the fractures are represented by probability distribution functions. It uses a geostatistical approach to model small-scale fractures, which can be contributing to local vertical heterogeneity.

In the DFN model, each fracture surface has individual attributes of permeability, compressibility, and aperture. The size, spatial location, intensity, and orientation of these surfaces are important and accounted for. Three main parameters are estimated to run the DFN model: the fracture distribution, geometry, and orientation. Because of the amount of information available at a well location, the DFN workflow and especially the identification of the fracture length and aperture have been developed to optimize the use of the well data. The key innovative points are the fracture length estimation from the borehole images and the fracture length/aperture relationship analysis to estimate the aperture of the individual fracture plane generated by the DFN.

How to optimize the identification of these three main parameters?

Fracture Distribution

A correct fracture density measurement is crucial in the DFN model generation, to be able to quantify the fracture intensity in a 3D grid. The fracture modeling results (Figure 8) can be used as input for the DFN model to define the density distribution. This property, described earlier, is computed from optimized fracture intensity curves from the well data and optimized fracture drivers from 3D seismic data (combined with other fracture drivers if available).

Fracture Geometry

In fractured basement reservoirs, one of the most challenging parameters to define for the DFN model is the fracture geometry, which includes the length distributions. To reduce the uncertainty in the evaluation of this parameter, an innovative method has been tested. It consists of statistical modeling of fracture extensions from borehole image logs. The mean fracture length can be estimated from fracture intersections statistics on borehole images.

Fracture Orientation

Finally, the orientation of the fractures in terms of dip angle and azimuth is defined according to the well data; the choice of the distribution is done on the stereonet of the sets of potential flow contributing fractures with specific orientation. A different orientation is defined for each fracture set.

Aperture is the most widely relied on measure for fracture "openness" which again is related to fluid flow and permeability. However, it is an uncertain parameter which is investigated for each reservoir individually. The aperture used in the model is based mainly on borehole images interpretation and fracture aperture computation from laterolog resistivity. The individual fracture permeability relies on the data available in the basement reservoirs and is calibrated to production data/flow measurements and to well tests when they are available or is related to the "cubic law" if no other measures are available.

DFN Upscaling

A DFN model is made with some fracture network attributes, as described above. However, for practical purposes in dynamic reservoir models, these are not useful until they are upscaled into the required grid properties that can be used for simulation.

Two methods are used for upscaling the permeability. The method proposed by Oda relies primarily on the geometry of the DFN to build the permeability tensor. It is fast and yields satisfactory values, but it generally needs to be calibrated to reproduce effective properties that have been independently derived. It is based on the total area of fractures in each cell. The second method is flow-based upscaling, which uses a finite element code to run three small-scale flow simulations per coarse cell directly on the DFN model. It is much slower but provides accurate results, and also provides the permeability tensor.

Fracture intensity model, porosity and permeability models can finally be used together to accurately predict new well targets (Figure 10) and the flow rates and recovery of prospective wells in fractured basement reservoirs.

Conclusion

Continuous fracture modeling relies on robust and consistent borehole image interpretation of fractures. This is achieved first by a readily accomplished classification of fractures into drilling-induced and natural fractures. The next step is to identify the fractures that contribute to flow based on fracture aperture and connectivity criteria. Based on this optimized fracture indicator, seismic poststack attributes are analyzed as potential fracture drivers.

The fracture models presented here also use geomechanical methods to predict the field-scale distribution of fractures that affect flow. The methodology for the geomechanical model includes different steps: (1) model configuration (fault geometry, tectonic load, rock properties, and boundary conditions), (2) 3D model validation, (3) boundary condition calibration (comparison with well data), and 4) prediction of the fractures associated with the main tectonic events. By modeling the physical processes responsible for fractures, more meaningful and realistic fracture systems can be predicted. This additional approach is also especially useful in fractured basement reservoirs with low quality of seismic data.

This workflow identifies the potential flow-contributing fractures by integrating borehole geology, petrophysical analyses, and seismic data. In addition, this solution provides a specific method to evaluate the fracture distribution, geometry, and orientation to match the well data and to obtain a realistic statistical image of the fracture network representing the subsurface.

Finally, the integrated approach of DFN and IFM modeling allows the analyst to improve the realistic representation of complex fracture system geometry and connectivity. It is a stochastic representation that can be used to estimate the uncertainty and the heterogeneity of the output variables (fracture porosity, permeability, etc.). Since the input parameters (fracture density, orientation) are 3D properties, it also captures the variability of these parameters at the reservoir scale.

In hydrocarbon reservoirs, fracture reactivation can have a significant effect on flow properties. Prediction of fracture reactivation (opening and shearing) under the current stress field can be performed with this workflow.

Acknowledgements

We wish to thank Alexis Carrillat, Arnaud Etchecopar, Josselin Kherroubi, Frantz and Laurent Maerten (Schlumberger, France) for their fruitful discussions and scientific support.

References

Bourne, S.J., and E.J.M. Willemse, 2001, Elastic Stress Control on the Pattern of Tensile Fracturing around a Small Fault Network at Nash Point, UK: Journal of Structural Geology, v. 23, p. 1753-1770.

Bourne, S.J, F. Brauckmann, L. Rijkels, B.J. Stephenson, A. Weber, and E.J.M. Willemse, 2000, Predictive Modelling of Naturally Fractured Reservoirs using Geomechanics and Flow Simulation: Paper ADIPEC 0911 presented at the 9th Abu Dhabi International Petroleum Exhibition and Conference, Abu Dhabi, U.A.E., 10 p.

Donald, J.A., and T.R. Bratton, 2006, Advancements in Acoustic Techniques for Evaluating Open Natural Fractures: SPWLA, 47th Annual Logging Symposium, Petrophysics Houston, v. 47/2, p. 156-157.

Endo, T., K. Tezuka, T. Fukushima, A. Brie, H. Mikada, and M. Miyairi, 1998, Fracture Evaluation from Inversion of Stoneley Transmission and Reflections: Proceedings of the Fourth SEGJ/SEG/ASEG International Symposium – Fracture Imaging – SEG Japan, p. 389-394.

Faivre, O., 1993, Fracture Evaluation from Quantitative Azimuthal Resistivities: SPE Paper 26434, 14 p.

Le, Van Hung, S. Farag, C. Mas, P.D. Maizeret, B. Li, and T. Dang, 2009, Advances in Granitic Basement Reservoir Evaluation:

Li, B., J. Guttormsen, T.V. Hoi, V. Duc Nguyen, 2004, Characterizing Permeability of the Fracture Basement Reservoirs: SPE Paper 88478, 11 p.

Luthi, S.M., 2005, Fractured Reservoir Analysis Using Modern Geophysical Well Techniques: Application to basement reservoirs in Vietnam: *in* P.K. Harvey, T.S. Brewer, P.A. Pezard, and V.A. Petrov, (eds), Petrophysical Properties of Crystalline Rocks: Geological Society, London, Special Publication, v. 240, p. 95-106.

Maerten, F., 2010, Geomechanics to solve geological structure issues: Forward, inverse and restoration modeling: Thesis/PhD, University of Montpelier II, France, 450 p.

Maerten, L., 2000, Variation in slip on intersection of normal faults: Implications for paleostress inversion: Journal of Geophysical Research, v. 105/25, p. 553-565.

Maerten, L., P. Gillespie, and J.M. Daniel, 2006, 3-D geomechanical modeling for constraint of subseismic fault simulation: AAPG Bulletin, v. 90/9, p. 1337-1358.

Maerten, L., E.J.M. Willemse, D.D. Pollard, and K. Rawnsley, 1999, Slip distributions on intersecting normal faults: Journal of Structural Geology, v. 21. P. 259-271.

Narr, W., D.W. Schechter, and L.B. Thompson, 2006, Naturally Fractured Reservoir Characterization: SPE Bookstore, 115 p.

Nelson, R.A., 2001, Geologic Analysis of Naturally Fractured Reservoirs, 2nd Edition: Gulf Professional Publishing Co., Boston, 332 p.

Oda, M., 1985, Permeability Tensor for Discontinuous Rock Masses: Geotechniques, v. 35, p. 483-495.

Randen, T., S.I. Pedersen, and L. Sonneland, 2001, Automatic Extraction of Fault Surfaces from Three-Dimensional Seismic Data: Extended Abstracts of 71st SEG Annual International Meeting, p. 551-554.

Sibbit, A., 1995, Quantifying Porosity and Estimating Permeability from Well Logs in Fractured Basement Reservoirs: SPE Paper 30157, 8 p.

Souche, L., J. Kherroubi, M. Rotschi, and S. Quental, 2009, A Dual Representation for Multiscale Fracture Characterization and Modeling: AAPG Search and Discovery Article #90090. Web accessed 11 December 2012. http://www.searchanddiscovery.com/abstracts/html/2009/annual/abstracts/souche.htm

Tamagawa, T., and D.D. Pollard, 2008, Fracture permeability created by perturbed stress fields around active faults in a fractured basement reservoir: AAPG Bulletin v. 92/6, p. 743-764.

Tamagawa, T., and K. Tezuka, 2004, Validation of Clustering of Fractures in Discrete Fracture Network Model by Using Fracture Density Distribution along Boreholes: SPE Paper 90342, 10 p.

Tandom, P.M., N.H. Ngo, H.D. Tjia, and P.M. Lloyd, 1999, Identifying and Evaluating Producing Horizons in Fractured Basement: SPE Paper 57324, 16 p.

Wang, H.M., L.C. Shen, G.J. Zhang, 1998, Dual Laterolog Response in 3-D Environments: Transactions of the SPWLA Annual Logging Symposium, v. 39, Paper X, 13 p.

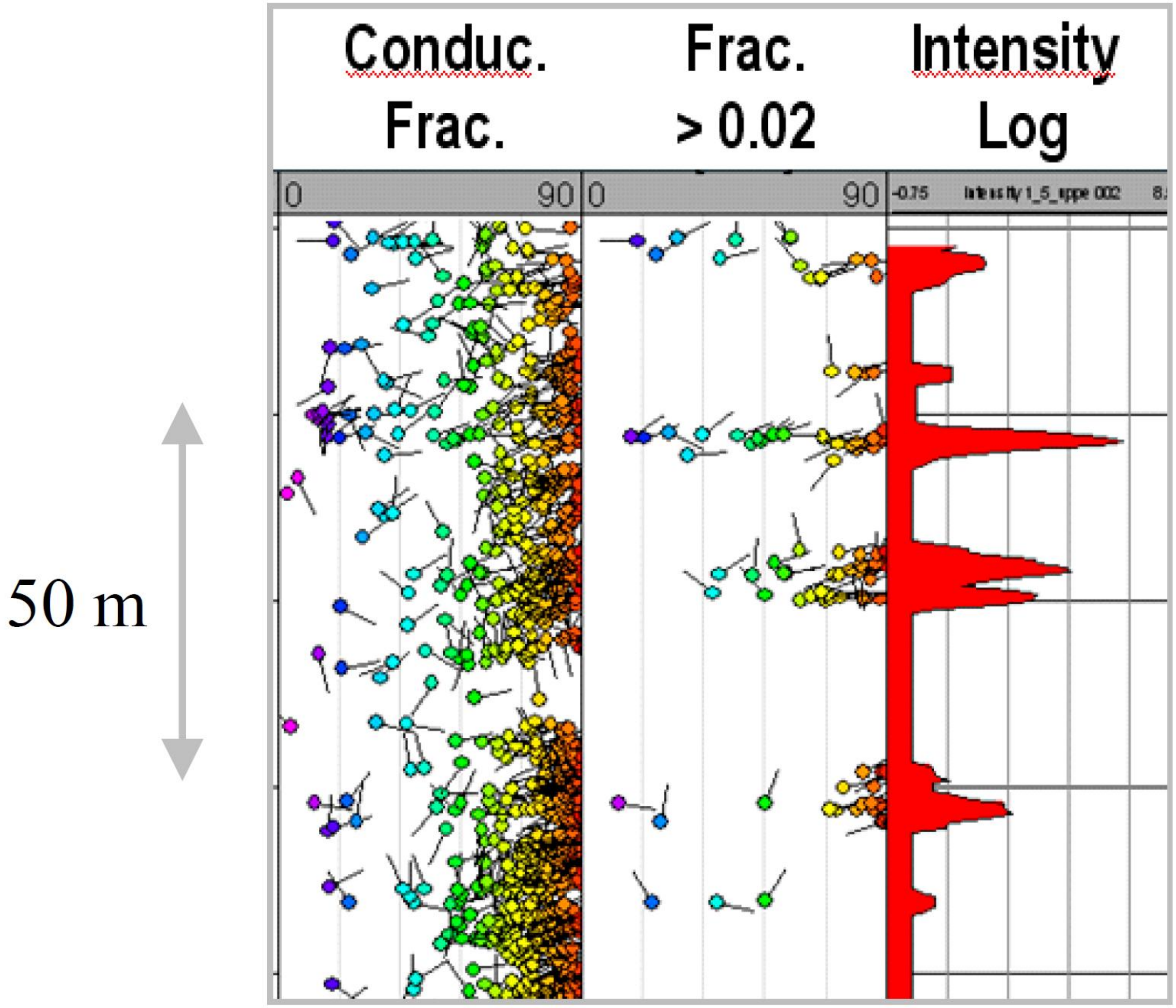

Figure 1. The full set of fractures in fractured basement reservoirs is not contributing to the flow. One part can contribute to the storage capacity and the other part can contribute to the flow. To optimize new well targets, the objective is to identify the flow-contributing fractures. In this example, tadpoles of all the conductive fractures picked from borehole images are represented on the track 1, and the tadpoles of the fractures which contribute to the flow are represented on the track 2. From this last set of fractures, a fracture intensity curve is computed (track 3). The fracture intensity (called also P32) is used as input for the 3D fracture modeling.

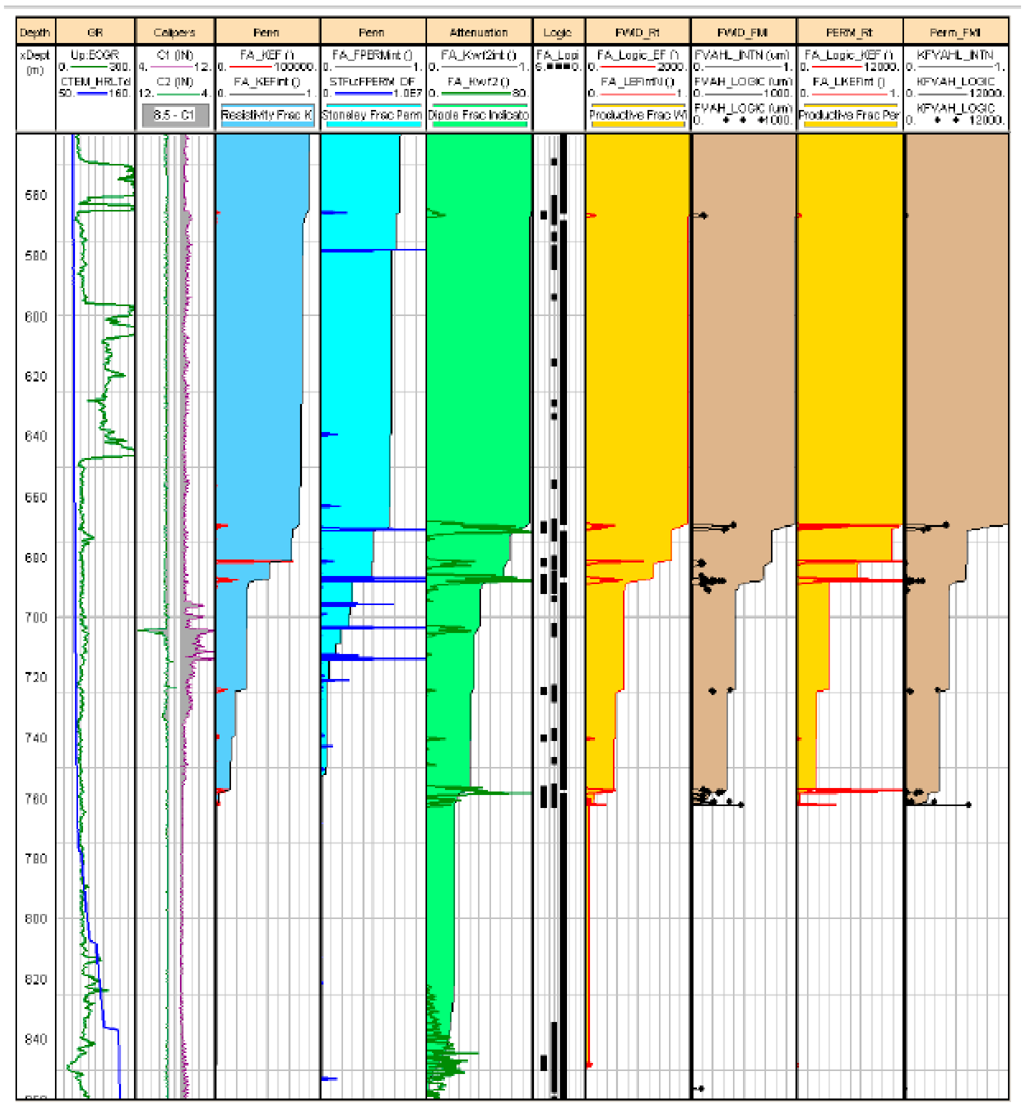

Figure 2. All measurements sensitive to fractures are prone to false positive fracture indications, but rarely to false negative indications. They also have different sensitivities to other factors such as the borehole condition or lithology. In zones where all the indicators agree, the fractures are likely to be open and permeable. In this case the interpretation predicts that most of the production should come from three main intervals: (1) 665 to 690 m, (2) ~725 m, (3) ~760 m with the larger portion coming from the first zone. In tracks 7 and 8 the filtered fracture apertures from resistivity (red curve) and image logs (black dots) are respectively presented. Tracks 9 and 10 show the permeability computed using the apertures (Endo et al., 1998).

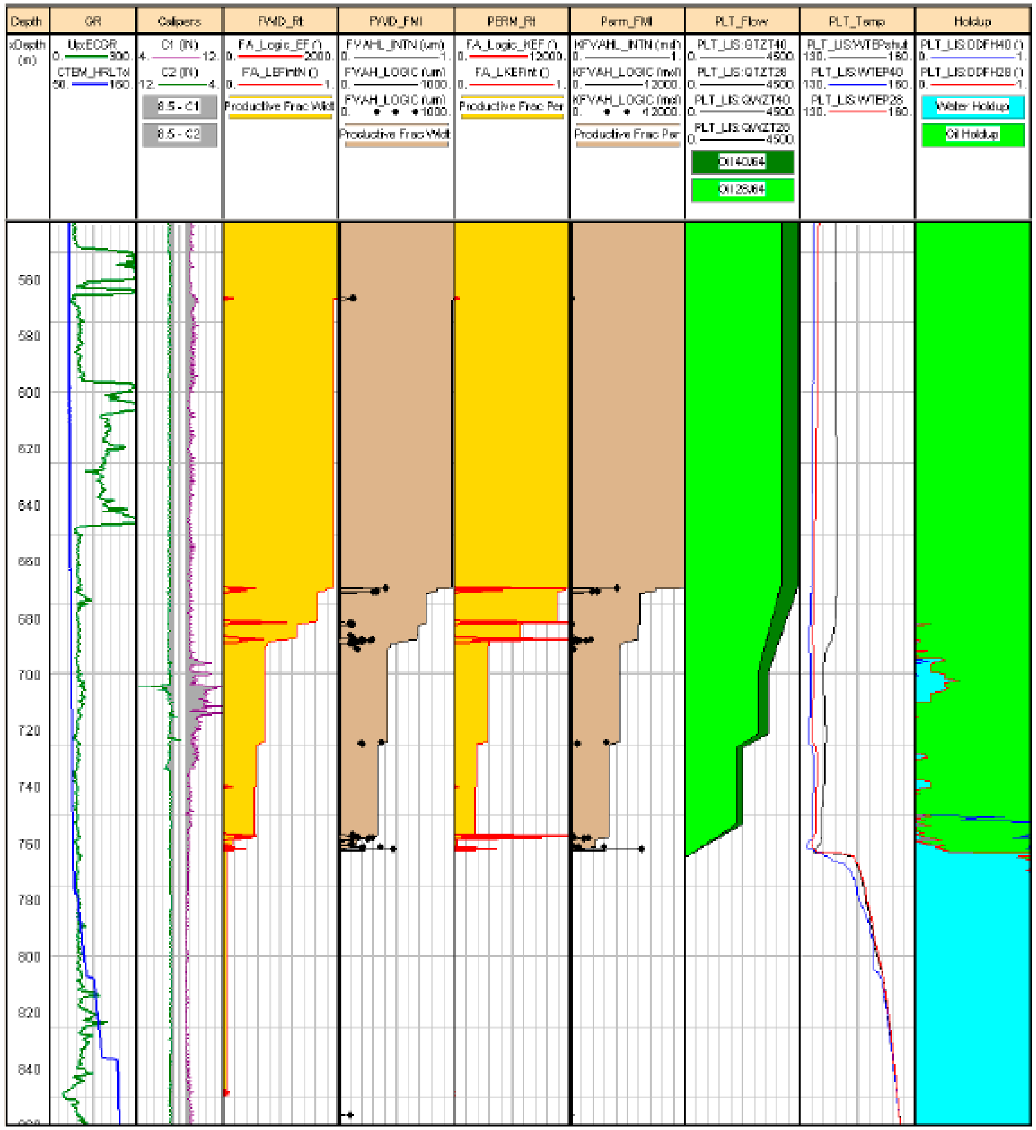

Figure 3. Production logs are compared to the log interpretation. Two-phase flow is observed only at the bottom most fractured zone (760 m). The shallowest water is observed at 700 m during the 28/64 inch flowing survey. This is trapped water due to wash out at that depth. The major entry points are correctly predicted by the static log interpretation. However, the relative contributions are different with zones 2 and 3 providing most of the production. This shows that fracture aperture is not the only factor affecting the production rate. The degree of connectivity to the rest of the reservoir, and fracture geometry, are also important factors (Endo et al., 1998).

	Fracture intensity Method 1	Fracture indicator from resistivity Method 2	P33 Method 3
Fracture intensity Method 1	1	0.8	0.8
Fracture indicator from resistivity Method 2	0.8	1	0.96
P33 Method 3	0.8	0.96	1

Figure 4. The fracture indicators computed by the different techniques are first compared qualitatively and then quantitatively. This example from a well in fractured basement from Vietnam correlates three fracture indicators: (1) fracture intensity computed from the comparison between borehole images, sonic data, production data/mud losses/gas show, (2) the fracture intensity computed from the laterolog resistivity, and (3) the porosity (P33) computed from the borehole images. The minimum correlation coefficients are 0.8.

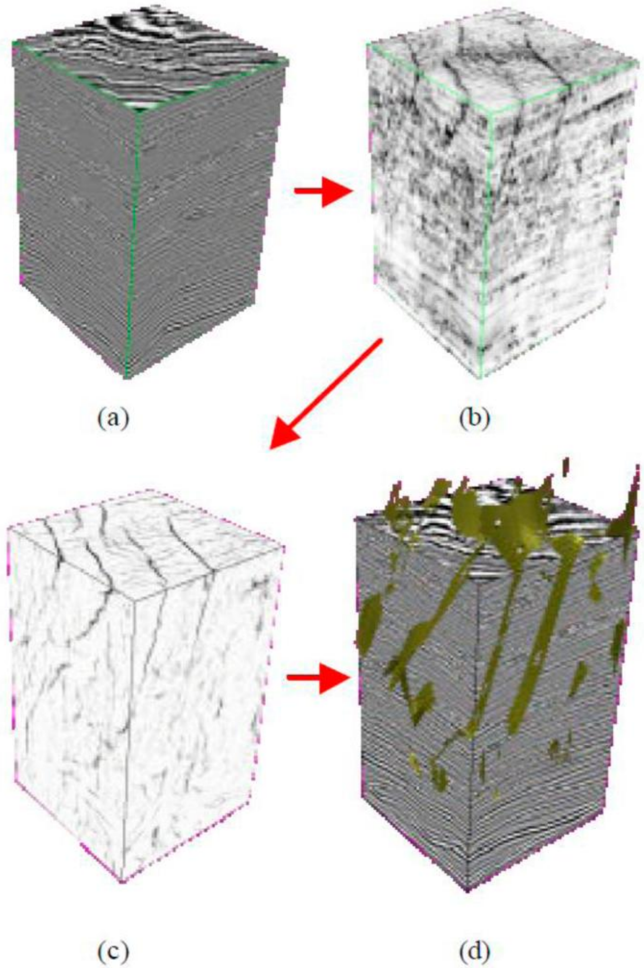

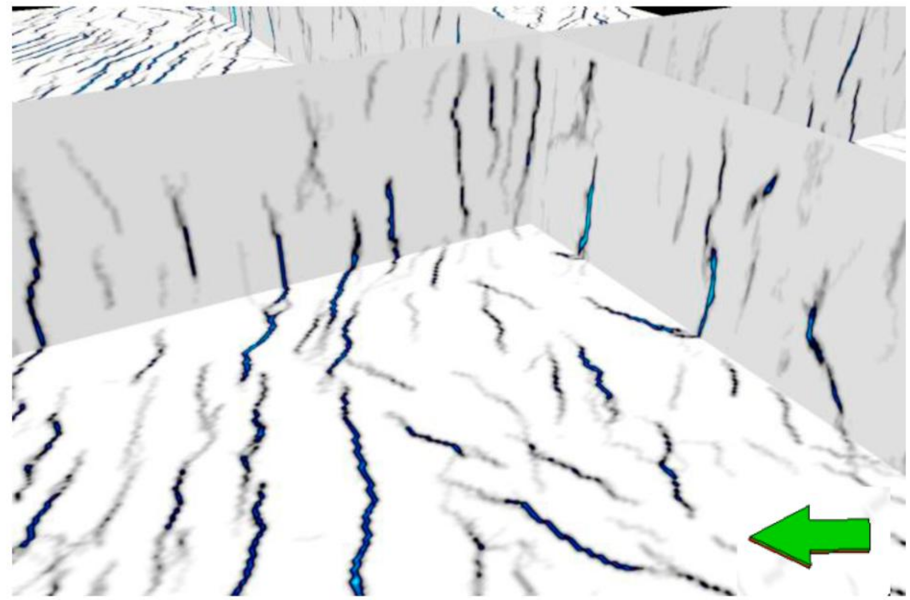

Figure 5. Ant-tracking workflow. The first step enhances the spatial discontinuities in the seismic data (fault attribute generation), and the second step significantly improves the fault attributes by suppressing noise and remains of non-faulting events. This is achieved by the cooperative behavior of thousands of “artificial ants”. In the sketch above, one or more attribute cubes (b) is generated from the seismic cube (a). The attribute is then conditioned, and from the resulting cube (c), the fault surfaces are extracted as separate objects (d). An example from fractured basement reservoir from Vietnam is presented on the right.

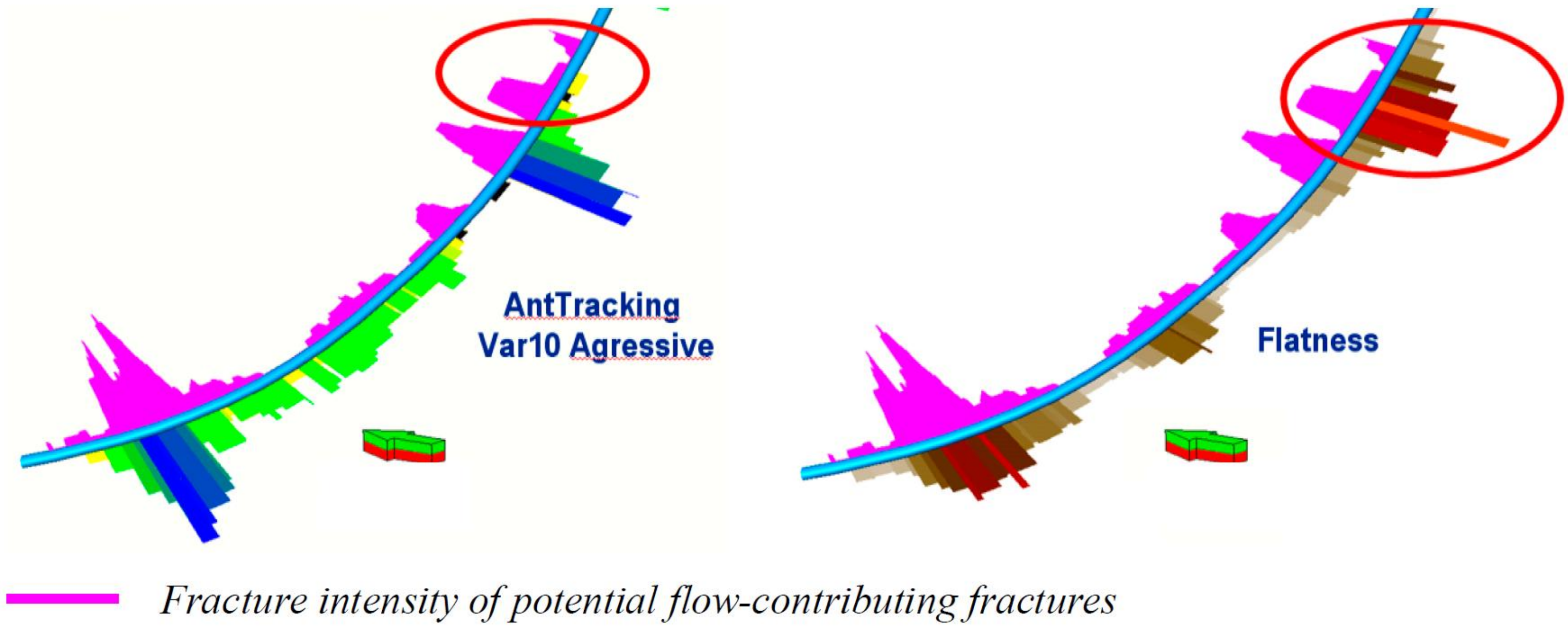

	Chaos	Flatness	T*attenuation	AntTracking
Intensity – 10	0.25	0.52	0.22	0.67
Intensity – 15	0.27	0.54	0.24	0.70
Intensity - 20	0.29	0.60	0.25	0.72

Figure 6. With this approach of a CFM workflow, an optimized set of key seismic attributes is identified qualitatively along the well path (top) and quantitatively via correlation coefficient analysis (bottom). In this example from fractured basement reservoirs, the ant tracking and flatness attributes are the best fracture drivers. This set is then used to constrain the propagation of fracture intensity away from the wells.

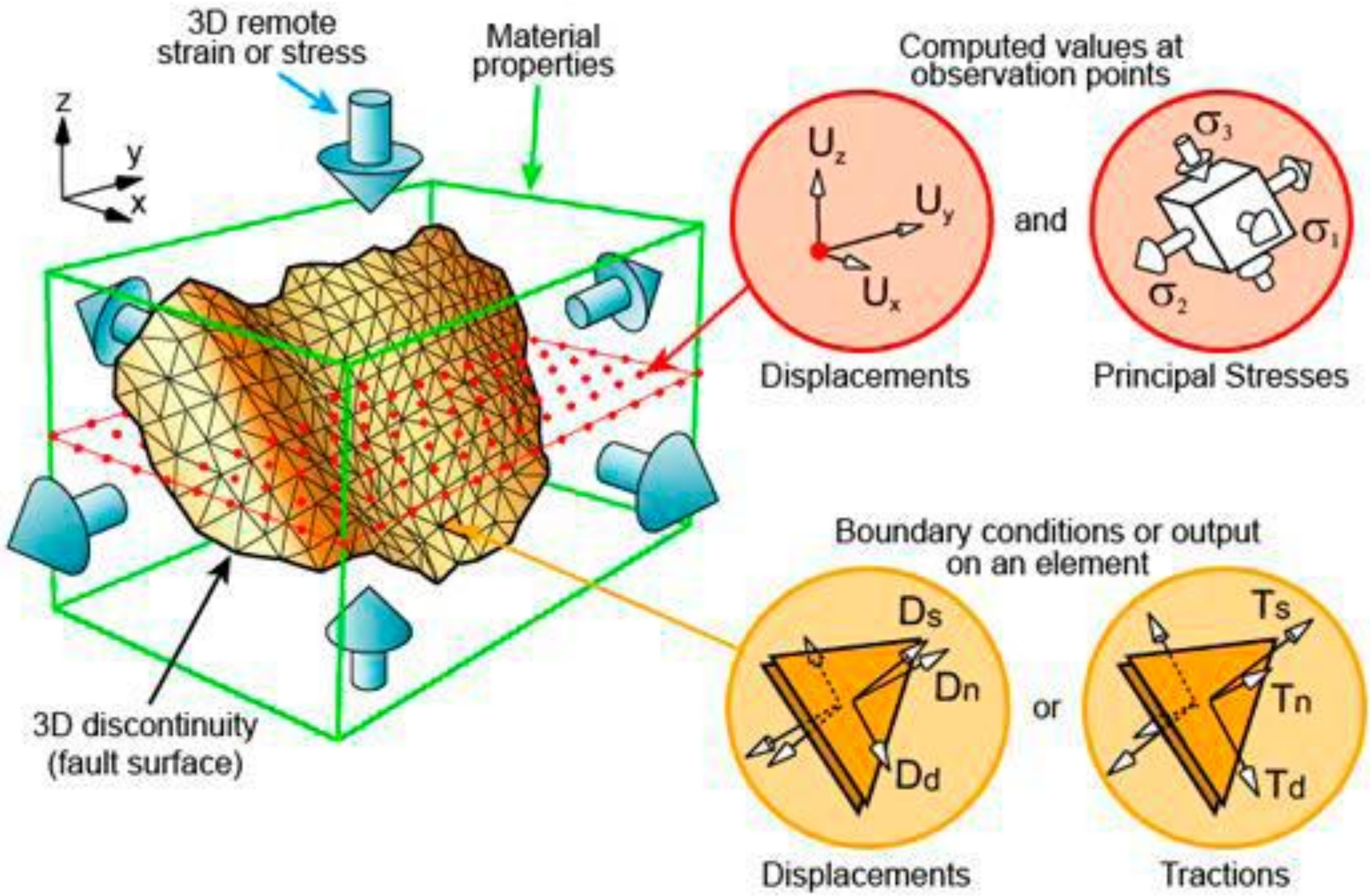

Figure 7. Construction of a complex fault geometry using triangular elements and schematic representation of a surrounding observation grid. Boundary conditions on triangular elements are a combination of displacement and traction. At each observation point, displacement, strain and stress can be computed as a post-process. Also shown is the 3D remote stress/strain (Maerten, 2010).

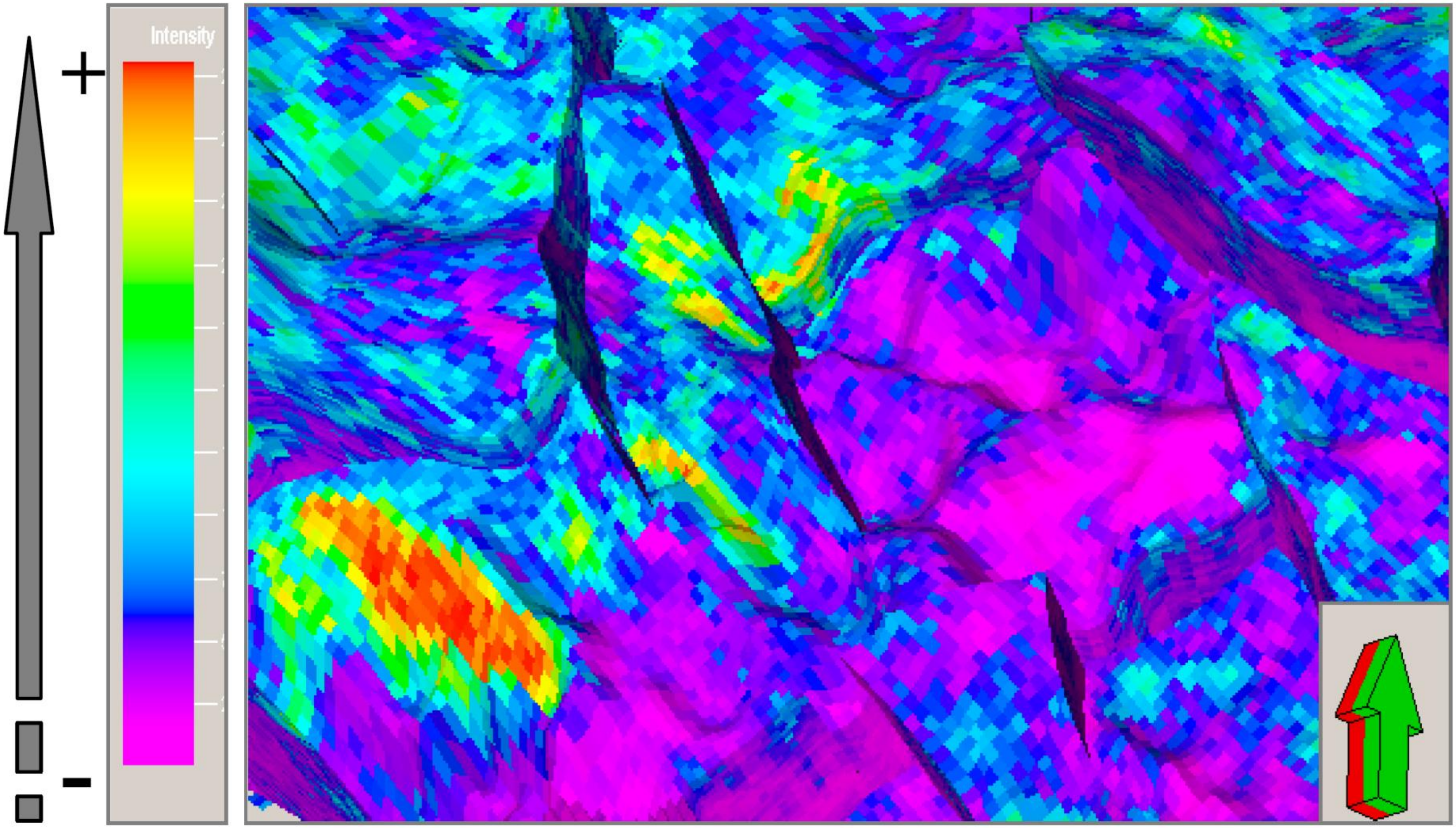

Figure 8. The result of the CFM is a 3D distribution of the flow-contributing fractures. From this 3D property, sweet spots with the highest fracture intensity can be highlighted. From the fractured basement example illustrated here, the purple color highlights the lowest intensity of potential flow-contributing fractures whereas the red color highlights the highest intensity. These red sweet spots are the main focus in planning new well targets.

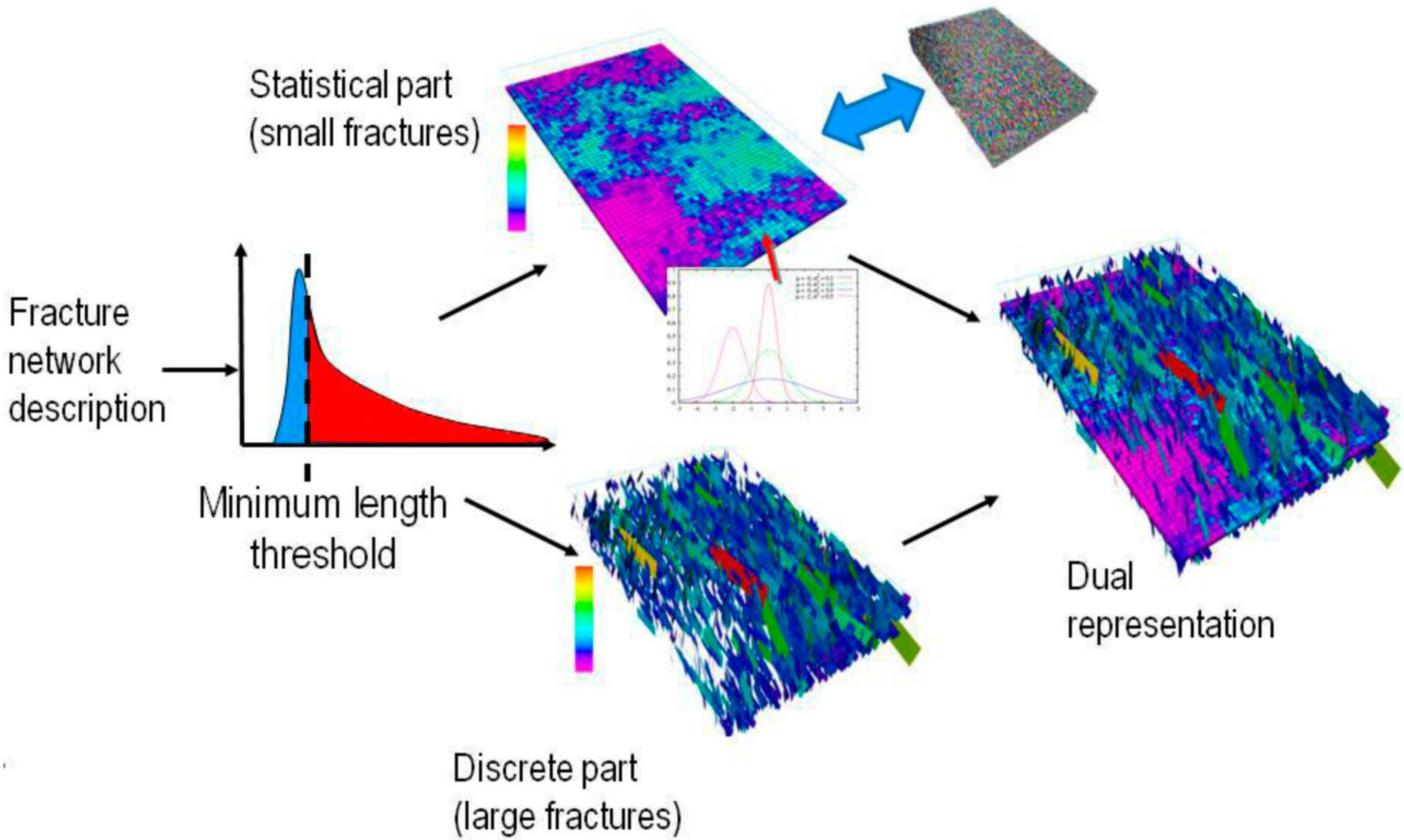

Figure 9. DFN and IFM modeling of large reservoir-scale and smaller-scale fractures (Souche et al., 2009). In the fracture network modeling process, there is a separation threshold that defines which fractures will be modeled discretely and implicitly. All fractures with length between zero and the given threshold will be modeled implicitly (as properties), while all fractures with lengths between threshold and the maximum length will be represented by discrete fractures (as planes).

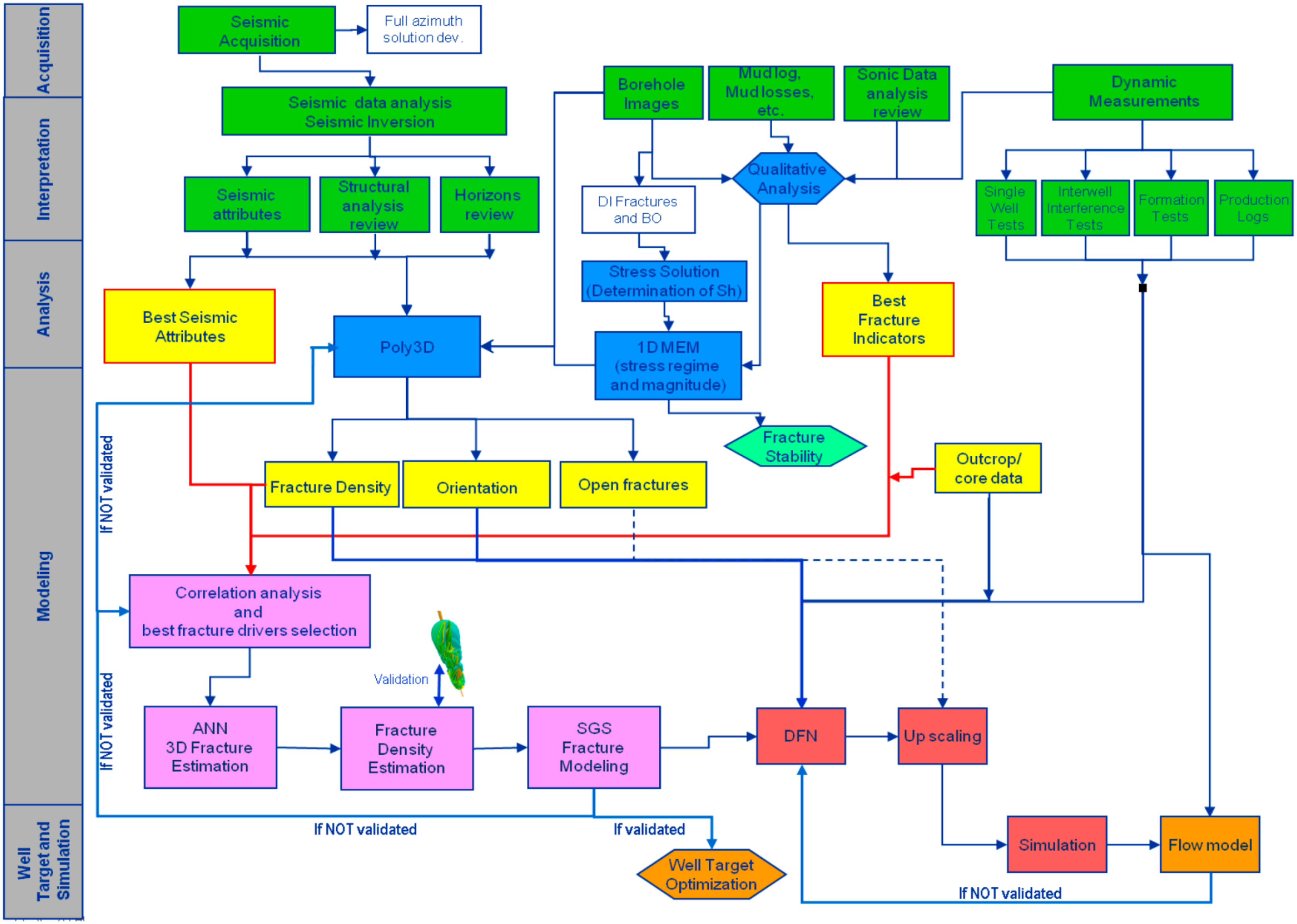

Figure 10. General fractured reservoir modeling workflow to identify new well target. It includes the following workflows: (1) best fracture indicators identification considering well data, production data, mud losses, and dynamic data, (2) best seismic attributes identification (green), (3) geomechanical property computation (blue), and (4) fracture modeling via CFM (pink) and DFN (red).